PHYSICAL REVIEW B **74**, 100402(R) (2006)

# Experimental evidence for the role of nonuniform modes in the asymmetric magnetization reversal of a Ni/NiO system

D. T. Dekadjevi,[1,*] A. Suvorova,[2] S. Pogossian,[1] D. Spenato,[1] and J. Ben Youssef[1]
[1]*Laboratoire de Magnetisme de Bretagne, Department of Physics, CNRS-UBO, 29285 Brest Cedex 3, France*
[2]*Centre for Microscopy and Microanalysis, University of Western Australia, Crawley, Western Australia 6009, Australia*
(Received 29 July 2006; published 25 September 2006)

Experimental evidence for the relevance of nonuniform reversal modes to asymmetric magnetization reversal is shown in a Ni/NiO polycrystalline system. The angular dependence of the asymmetry, exchange bias, and coercive field is studied as a function of NiO structural disorder and thickness. The contribution of nonuniform reversal modes and coherent rotation to the magnetization reversal depends on the angle between the applied field and the ferromagnetic easy axis. We observe two distinct critical angles revealing the significant role of nonuniform magnetization reversal in the asymmetry and its angular dependence.

DOI: 10.1103/PhysRevB.74.100402 PACS number(s): 75.60.Jk, 75.50.Ee, 75.70.Cn

Uniaxial anisotropic properties in magnetism open a world of hysteretic behavior. Over recent decades, a new kind of anisotropy named unidirectional (or exchange) anisotropy has been discovered[1,2] and thoroughly studied for fundamental understanding of magnetization reversal and for applied use in read heads.[3,4] This exchange anisotropy is observed in ferromagnetic (F)/antiferromagnetic (AF) bilayers and revealed by the hysteresis loop shift along the field axis ($H_e$) and the coercive field ($H_c$) enhancement. Experimental observations and theoretical predictions have shown that domain wall (DW) formation in the ferromagnet and/or in the antiferromagnet should be considered in the reversal mechanism in order to obtain a reasonable value for $H_e$.[5] Mauri *et al.* suggested the presence of parallel DWs at the interface.[6] $H_e$ would then depend on the energy stored in this wall. This model does not exhibit a coercive enhancement for a perfect system (no disorder or zero temperature). Defects within this DW are predicted to enhance the anisotropy locally and result in DW pinning leading to the $H_c$ enhancement.[7] Instead of a parallel DW proposed in those models, Malozemoff,[8] followed by Nowak *et al.*,[9] predicted that nonuniform magnetization reversal, via the creation of a multidomain structure in the AF, was a driving mechanism for exchange anisotropy. In the models, interfacial or AF bulk defects lead to a random field that breaks the AF layer into domains over its area. $H_e$ originates from the interfacial staggered spins, i.e., the nonreversible part of the interfacial spins. The $H_c$ enhancement originates from the reversible process driven by the AF uniaxial anisotropy that procures additional critical fields to hinder the DW motion in the F.[10,11]

The presence of domains in the magnetization reversal is associated with unusual properties of exchange bias systems. Among them, the asymmetric reversal of magnetization has recently received particular attention. This phenomenon is peculiar since it is not found in other hysteretic physical systems. It is experimentally observed by techniques sensitive not only to the magnetization strength but also to its vectorial character. These experiments have shown that magnetization reversal may be different on each side of the hysteresis loop, and this asymmetry would depend on the angle between the applied field and the F easy axis.[12–16] The contributions of coherent rotation and domain nucleation to the asymmetry and its angular dependence are outlined but their respective roles are still unclear. Recent studies have shown that features of the angular dependence of the asymmetry can be reproduced by coherent rotation reversal.[15,17] Their results support the nonrelevance of the nonuniform magnetization reversal, i.e., DW formation, to the asymmetry and its angular dependence. However, Beckmann *et al.* have predicted the relevance of domains using numerical simulations based on the domain state model.[18] The dependence of the asymmetry on the AF structural ordering has not yet been probed experimentally.

In this Rapid Communication, we present experimental evidence for the AF domain contribution in the asymmetric Ni/NiO magnetization reversal. We modified the NiO magnetic properties through changes in its structural ordering to understand the magnetization reversal mechanism. A structural study of [glass/Ni/NiO] bilayers in real and reciprocal space is first presented. Following this, the unidirectional and $H_c$ evolutions as a function of the NiO disorder and thickness are probed to determine the magnetization reversal properties. Finally, the domain contribution to the appearance of the asymmetry is shown via a systematic study of the angular dependence of magnetization. Structures were grown on glass substrates by rf sputtering under a 300 Oe magnetic field and with a base pressure of $10^{-7}$ mbar. The NiO layers were obtained from the sputtering of a $Ni_1O_1$ target. They were grown at different argon gas pressure ($P$) to modify the structural ordering. In this Rapid Communication, $NiO_P$ corresponds to a NiO layer grown at $P \times 10^{-3}$ mbar. Compositional and structural characterization were performed using energy-filtered transmission electron microscopy (EFTEM), transmission electron microscopy (TEM), and x-ray reflectometry (XRR) and diffraction (XRD) techniques. Magnetic measurements were performed at room temperature using a vectorial vibrating-sample magnetometer (VSM).

TEM studies of the Ni/NiO structure in cross-sectional projection showed the polycrystalline nature of both layers. It should be noted that the NiO polycrystalline nature shown by TEM is confirmed by a 25° wide rocking curve on the (111) peak, for each value of pressure. Figure 1, obtained on [Ni(53 Å)/$NiO_4$(700 Å)], shows NiO grains with a rectangular shape, having width 190±40 Å and height 400 Å. The Ni grains also had a rectangular shape with height equal to thickness and a 40 Å width. The chemical information was

 

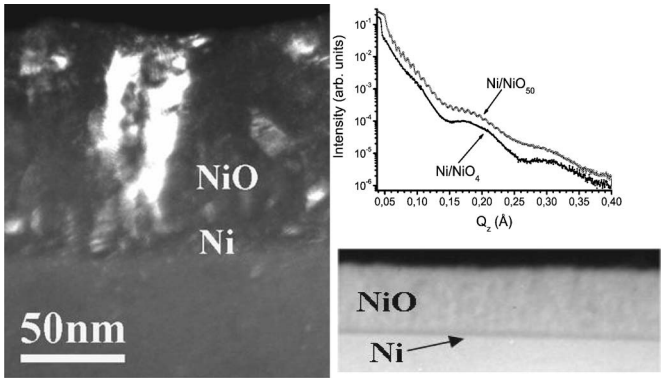


FIG. 1. Left: TEM dark-field image of $[Ni(53\ Å)/NiO_{50}(700\ Å)]$. Top right: XRR spectra of $[Ni(53\ Å)/NiO_{50}(700\ Å)]$ and $[Ni(53\ Å)/NiO_4(700\ Å)]$. Bottom right: energy-selected image of $[Ni(53\ Å)/NiO_{50}(700\ Å)]$ obtained at 400 eV energy loss (Ni $L_{2,3}$ edge) with energy slit 40 eV.

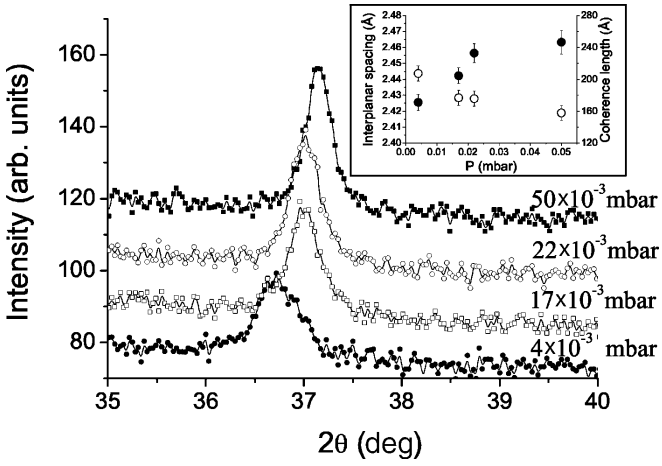


FIG. 2. High-angle x-ray diffraction scans as a function of the argon sputtering gas pressure $P$ in $[Ni(53\ Å)/NiO_P(700\ Å)]$. The argon pressure $P$ is indicated at the tail of each curve. In the inset, interplanar spacing (open circle) and coherence length (filled circle) are shown as a function of $P$.

visualized by generating EFTEM images of constituent elements. Ni elemental maps, O elemental maps, and energy-selected images demonstrate continuous coverage within the NiO films and a well-defined Ni layer as shown in Fig. 1. The reliability of the EFTEM information depended on the spatial resolution of this technique, ~20 Å in these experiments. Consequently, short-range disorder such as point defects was undetectable. However, diffraction techniques give information about such defects as they lead to nonuniform strain.[19]. XRD measurements at $\lambda = 1.542$ Å and from Bragg planes parallel to the surface were performed on all samples and for all $P$. $[Ni(53\ Å)/NiO_P(700\ Å)]$ diffraction spectra are shown in Fig. 2. Interplanar spacings were determined from the positions of the Bragg peaks. Out-of-plane coherence lengths were obtained by inserting the values of full width at half maximum into the Scherrer equation. In our system, $P$ reduction resulted in an enhancement of the uniform strain shown by the evolution of the interplanar spacings in the inset of Fig. 2. For all $P$, the out-of-plane coherence length was smaller than the crystallite height observed by TEM. In the absence of nonuniform strain, the coherence length would be equal to the crystallite height in our measurements.[19] This shows that nonuniform strain is present and is increased when $P$ is reduced. It should be noted that identical measurements were obtained whether NiO was grown on Ni or glass. This shows that the structural change induced by $P$ was not contained at the interface but was an internal property of the NiO layer.

In addition to the crystalline ordering, we probed the evolution of the interfacial width and the density, by taking x-ray reflectivity measurements. In these measurements, the critical wave vector depends on the electronic density of the top layers. The amplitude of the oscillations, named Kiessig fringes (KF), depends on the electronic density profile in the structure.[19] Figure 1 shows the specular reflectivity data obtained for 700-Å-thick NiO grown at the minimum and maximum $P$. At the highest pressure, well-defined KF arose from Ni and NiO layers, indicating an abrupt interface and a low surface roughness. When $P$ was decreased, the high-frequency KF arising from the NiO layer were attenuated, indicating changes in the electronic density, whereas the low-frequency ones arising from the Ni layer were maintained. Showing a decrease in the NiO electronic density with the reduction of $P$, i.e., an increase of the O content with the reduction of $P$, the critical wave vector is changing from the NiO value (0.051 $Å^{-1}$) toward lower values when $P$ is decreased. $Ni_1O_1$ is obtained for an argon pressure of $50 \times 10^{-3}$ mbar (i.e., $P=50$). It should be noted that the evolution of the NiO critical wave vector and fringe amplitude with $P$ was identical for a single NiO layer. This shows that those structural changes probed by XRR were not at the interface but were an internal property of the NiO layer.

To summarize, the evolution of the electronic density and uniform strain with the reduction of $P$ shows an increase of the oxygen content in the NiO layer. $Ni_1O_1$ is obtained at the highest pressure. The evolution of the out-of-plane coherence length with the reduction of $P$ shows an increase of defects with the reduction of $P$. The $[Ni/NiO_P]$ magnetic properties are now studied to understand the driving mechanism of the exchange anisotropy properties.

Magnetization reversal loops, with the field applied along the F easy axis, were recorded simultaneously along the longitudinal and transverse directions using the VSM. The easy-axis loop along the longitudinal direction exhibits a symmetric and shifted hysteresis loop above a given NiO thickness. Furthermore, no magnetization is detected along the transverse direction. Polarized neutron reflectivity measurements, not presented here, confirm the absence of a transverse component of magnetization when the field is applied along the easy axis. Such observations rule out coherent rotation reversal when the field is applied along the easy axis. The nucleation of DWs perpendicular to the interface must be taken into account to understand the exchange properties in our system. A planar-type DW could explain the exchange anisotropy properties only locally.

The influence of the NiO thickness and structural disorder on the unidirectional and $H_c$ is shown in Fig. 3. For all disorder states within the AF, the presence of a critical thickness

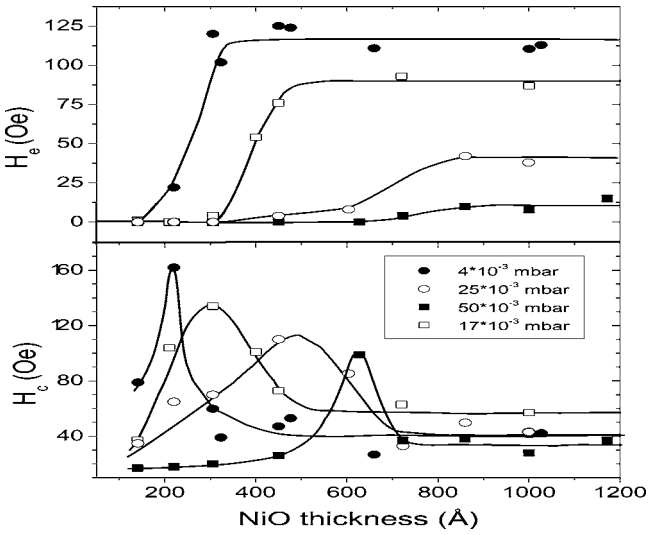


FIG. 3. $H_c$ and $H_e$ evolution with $P$ and NiO thickness. The continuous lines are guides.

$t_c$ is shown. For such a thickness, $H_e$ differs from zero to reach a saturated value and $H_c$ is maximum. Within a random-field-type model, $H_e$ differs from zero when the AF anisotropy energy is sufficiently large to hold nonreversible AF spins in place.[10] In models including the formation of a parallel DW at the interface, $H_e$ differs from zero if the thickness is greater than the DW width.[6,20] Figure 3 shows that disorder introduced within the AF results in an increase of $H_e$ and in the $H_c$ maximum. Such disorder effects on $H_e$ and $H_c$ are explained in domain-state-type models, where disorder induces a random field, and in the modified Mauri model,[7] where disorder may induce local anisotropy enhancement. To understand the driving mechanism of the $H_e$ and $H_c$ evolution with the NiO thickness and disorder, one needs to distinguish between these two classes of model. We have probed the presence of a parallel DW by studying [Ni(53 Å)/$NiO_{50}$(100 Å)/$NiO_4$($t$)] trilayers as a function of

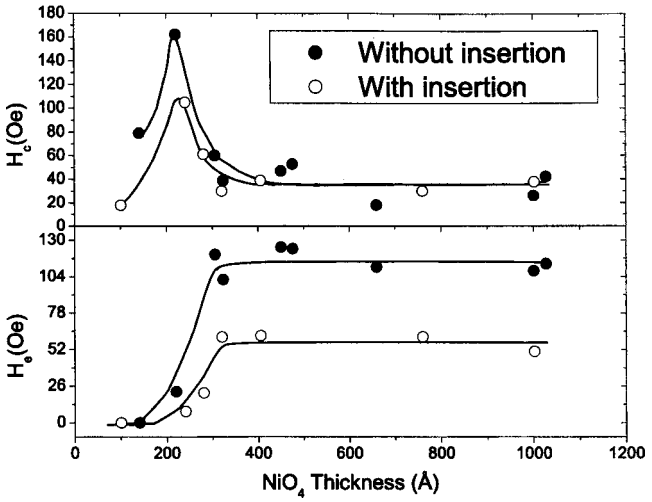


FIG. 4. $H_e$ and $H_c$ evolution with thickness in [Ni(53 Å)/$NiO_{50}$(100 Å)/$NiO_4$($t$)]. The continuous lines are guides.

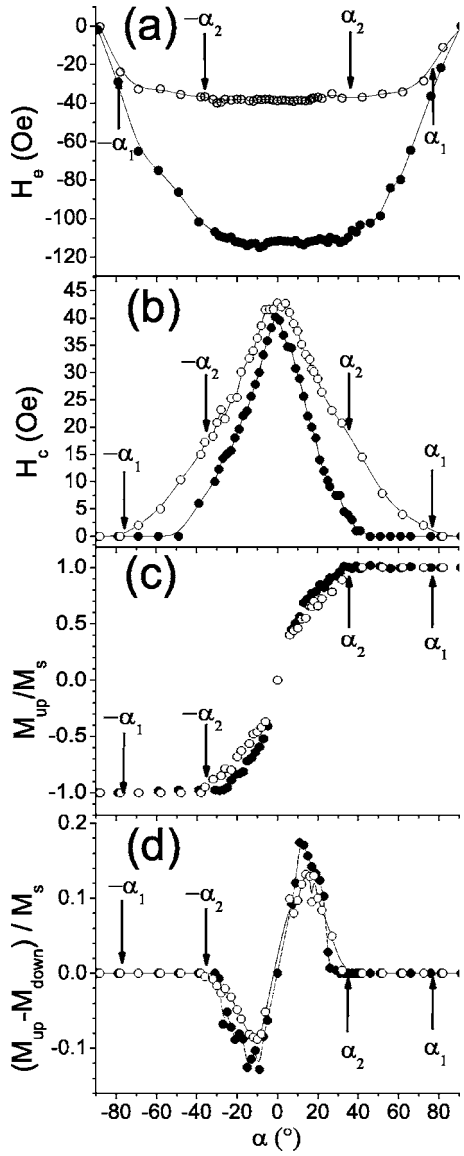


FIG. 5. Angular dependence of (a) $H_e$, (b) $H_c$, (c) normalized $M_{up}$, and (d) asymmetry of [Ni(53 Å)/$NiO_4$(1000 Å)] (filled circles) and [Ni(53 Å)/$NiO_{25}$(1000 Å)] (open circles). For clarity, critical angles $\alpha_1$ and $\alpha_2$ are drawn only for the [Ni(53 Å)/$NiO_{25}$(1000 Å)] sample.

$t_{NiO_4}$, the thickness of the NiO layer presenting the highest $H_e$. Figure 4 shows that the critical thickness is not modified by the insertion of the interfacial layer. However, the $H_e$ and $H_c$ maxima are reduced. If the parallel DW was responsible for the exchange anisotropy, $H_e$ would be proportional to the energy contained in the DW, i.e., proportional to $(AK_u)^{1/2}$, with $A$ being the exchange constant and $K_u$ the AF uniaxial anisotropy constant. The critical thickness will be proportional to the DW width, i.e., proportional to $(A/K_u)^{1/2}$. A change in the AF exchange or anisotropy constant will result in a change of both properties $t_c$ and $H_e$. In the case of a bilayer AF structure, the energy of the DW will be contained in both layers with contributions depending on the width of the wall.[21] The reduction of $H_e$ after insertion would show that part of the DW is contained in the first layer. In this case,

$t_c$ would be modified. The stability of $t_c$ with the important reduction of $H_e$ shows that parallel DWs do not drive the exchange anisotropy.

It should be noted that $H_e$ and the $H_c$ maximum have reduced values when there is insertion but not as low as in [Ni/$NiO_{50}$]. This confirms that, even though exchange anisotropy is an interface phenomenon, the bulk plays a significant role in our system. Even if the random field originates in interfacial defects, DWs have to propagate through the whole thickness. We observe no significant evolution of $H_c$ with disorder for thickness greater than $t_c$. This may explain the complexity of understanding the $H_c$ evolution in previous experimental studies where the AF thickness is fixed.[22,23]

We have undertaken a systematic study of the angular dependence of the magnetization reversal to probe the domain contribution. In particular, we measured the net transverse magnetization component on both sides of the hysteresis loop, at various angles. We quantify the asymmetry as $(M_{up}-M_{down})/M_s$ where $M_{up}$ ($M_{down}$) is the maximum of the transverse component for the increasing (decreasing) field branch, where $M_s$ is the saturated magnetization.

The angular dependence of [Ni(53 Å)/$NiO_4$(1000 Å)] and [Ni(53 Å)/$NiO_{25}$(1000 Å)] exhibit a first critical angle $\alpha_1$ corresponding to the onset of coercivity as shown in Fig. 5. At this angle, $M_{up}$ is equal to the saturated magnetization $M_s$ and the asymmetry is zero. The reversal is then a coherent rotation. Using the Stoner and Wohlfarth model, $\alpha_1$ is defined as $\arctan(2K_u/K_e)$ where $K_u$ is the uniaxial anisotropy constant determined from the hard axis loop and $K_e$ $(=H_eM_s)$ is the unidirectional anisotropy constant.[15] The predicted $\alpha_1$ value is 72° (47°) in [Ni(53 Å)/$NiO_{25}$(1000 Å)] ([Ni(53 Å)/$NiO_4$(1000 Å)]) and is in very good agreement with the observed experimental value. However, the onset of asymmetry occurs at a second critical angle $\alpha_2$ corresponding to the decrease of $(M_{up}/M_s)$. At this critical angle, nonuniform reversal, i.e., multidomain structure, is shown by such a decrease. Our results are different from that obtained using the Stoner and Wohlfarth model. In their model, the critical angle is the onset of the coercivity and asymmetry $(\alpha_1=\alpha_2)$. However, in our study, the coercivity vanishes after the asymmetry $(\alpha_1>\alpha_2)$. The coherent rotation mechanism fails to describe the features of our system and nonuniform reversal should be considered. It shows that the asymmetry of the magnetization reversal is found to be greater when the ratio $K_u/K_e$ decreases. Numerical simulations based on the domain state model have recently predicted that the nonuniform reversal mode leads to the asymmetry and its angular dependence.[18] Our experimental study supports such a prediction and outlines the relevance of domain formation in the asymmetry. Furthermore, we observe a 40% (55%) decrease of the $\alpha_2$ ($\alpha_1$) value when $P$ decreases from 25 to 4. These results show that $\alpha_2$ and $\alpha_1$ values are driven by identical physical properties such as NiO disorder. A recent study has shown that F parallel DW play a dominant role in the $FeF_2$/Ni asymmetric reversal.[24] Our study demonstrates that asymmetric reversal in polycrystalline Ni/NiO is not related to such a mechanism but depends on the nonuniform reversal modes driven by AF disorder. This experimental evidence outlines the need to include the AF structure to understand the asymmetric reversal. Such a structure has mostly been ignored in experimental studies of the asymmetric magnetization reversal.[15,24,25] We expect a deeper insight into the physics of exchange anisotropy from a comparison of these results with novel theoretical and experimental work studying asymmetric reversal properties and probing the key role of the AF structure.

In conclusion, exchange properties are influenced by the internal structure of the antiferromagnet that we modified by changing the NiO stoichiometry. The angular dependence of the exchange properties is not explained by the Stoner and Wohlfarth model as it exhibits two critical angles. The first angle corresponds to the onset of coercivity and the second to the onset of nonuniform reversal and asymmetry. The multidomain structure should be included in the reversal mechanism to understand the asymmetry of the magnetization reversal in the studied polycrystalline Ni/NiO structures.

We thank K. Garello and V. Castel for the VSM measurements and M. Viret for critical reading of the manuscript. We acknowledge the Rutherford Appleton Laboratory for the provision of neutrons and we would like to thank T. Charlton, R. M. Dagliesh, and S. Langridge for useful discussions and assistance in using the CRISP instrument.

*Electronic address: david.dekadjevi@univ-brest.fr

[1] W. H. Meiklejohn and C. P. Bean, Phys. Rev. **102**, 1413 (1956).
[2] W. H. Meiklejohn and C. P. Bean, Phys. Rev. **105**, 904 (1957).
[3] J. Nogues and I. K. Schuller, J. Magn. Magn. Mater. **192**, 203 (1999).
[4] A. E. Berkowitz and K. Takano, J. Magn. Magn. Mater. **200**, 552 (1999).
[5] C. H. Marrows *et al.*, Phys. Rev. B **66**, 024437 (2002).
[6] D. Mauri *et al.*, J. Appl. Phys. **62**, 3047 (1987).
[7] J. V. Kim and R. L. Stamps, Phys. Rev. B **71**, 094405 (2005).
[8] A. P. Malozemoff, Phys. Rev. B **35**, 3679 (1987).
[9] U. Nowak *et al.*, Phys. Rev. B **66**, 014430 (2002).
[10] A. Misra *et al.*, J. Appl. Phys. **95**, 1357 (2004).
[11] L. Zhang and S. Zhang, Phys. Rev. B **61**, R14897 (2000).
[12] M. R. Fitzsimmons *et al.*, Phys. Rev. Lett. **84**, 3986 (2000).
[13] P. Gogol *et al.*, J. Appl. Phys. **92**, 1458 (2002).
[14] E. Pina *et al.*, Phys. Rev. B **69**, 052402 (2004).
[15] J. Camarero *et al.*, Phys. Rev. Lett. **95**, 057204 (2005).
[16] L. Spinu *et al.*, Phys. Rev. B **68**, 220401(R) (2003).
[17] A. Tillmanns *et al.*, cond-mat/0509419 (unpublished).
[18] B. Beckmann *et al.*, Phys. Rev. Lett. **91**, 187201 (2003).
[19] P. F. Fewster, Rep. Prog. Phys. **59**, 1339 (1996).
[20] H. Xi and R. M. White, Phys. Rev. B **61**, 80 (2000).
[21] H. Kronmuller and M. Fahnle, *Micromagnetism and the Microstructure of Ferromagnetic Solids* (Cambridge University Press, Cambridge, U.K., 2003).
[22] R. Shan *et al.*, Phys. Rev. B **71**, 064402 (2005).
[23] L. Thomas *et al.*, J. Appl. Phys. **93**, 6838 (2003).
[24] Z. P. Li *et al.*, Phys. Rev. Lett. **96**, 217205 (2006).
[25] P. Blomqvist *et al.*, Phys. Rev. Lett. **94**, 107203 (2005).